

University of Texas Rio Grande Valley

ScholarWorks @ UTRGV

Chemistry Faculty Publications and
Presentations

College of Sciences

4-2020

Glutaminyl-tRNA Synthetase from *Pseudomonas aeruginosa*: Characterization, structure, and development as a screening platform

Yaritza Escamilla

Casey A. Hughes


Jan Abendroth

David M. Dranow

Samantha Balboa

See next page for additional authors

Follow this and additional works at: https://scholarworks.utrgv.edu/chem_fac

 Part of the [Chemistry Commons](#)

Authors

Yaritza Escamilla, Casey A. Hughes, Jan Abendroth, David M. Dranow, Samantha Balboa, Frank B. Dean, and James M. Bullard

Bullard James (Orcid ID: 0000-0002-3068-3717)

Glutaminyl-tRNA Synthetase from *Pseudomonas aeruginosa*: Characterization, Structure, and Development as a Screening Platform

Yaritza Escamilla¹, Casey A. Hughes^{1†}, Jan Abendroth^{2,3}, David M. Dranow^{2,3}, Samantha Balboa^{1‡}, Frank B. Dean¹, and James M. Bullard^{1*}

¹The University of Texas - RGV, Edinburg, TX 78541, ²Seattle Structural Genomics Center for Infectious Disease, Seattle, WA 98109, and ³UCB Biosciences, Bainbridge Island, WA, 98110

[†]Present address: Department of Biochemistry and Biophysics, College of Agriculture and Life Sciences, Texas A&M University, College Station, TX 77843

[‡]Present address: Department of Chemistry, College of Arts and Science, The University of North Carolina, Chapel Hill, NC 27599

*Corresponding author. Mailing address: Chemistry Department, ESCNE. 4.612, The University of Texas - RGV, 1201 W. University Drive, Edinburg, TX 78541.

This is the author manuscript accepted for publication and has undergone full peer review but has not been through the copyediting, typesetting, pagination and proofreading process, which may lead to differences between this version and the [Version of Record](#). Please cite this article as doi: [10.1002/pro.3800](https://doi.org/10.1002/pro.3800)

Phone: 956-665-2950 Mobile: 303-775-5100 Fax: 956-665-5006

E-mail: james.bullard@utrgv.edu; jmbullard.wa@gmail.com

Abstract

Pseudomonas aeruginosa has a high potential for developing resistance to multiple antibiotics. The gene (*glnS*) encoding glutamyl-tRNA synthetase (GlnRS) from *P. aeruginosa* was cloned and the resulting protein characterized. GlnRS was kinetically evaluated and the K_M and k_{cat}^{obs} , governing interactions with tRNA, were 1.0 μ M and 0.15 s^{-1} , respectively. The crystal structure of the α_2 form of *P. aeruginosa* GlnRS was solved to 1.9 Å resolution. The amino acid sequence and structure of *P. aeruginosa* GlnRS were analyzed and compared to that of GlnRS from *Escherichia coli*. Amino acids that interact with ATP, glutamine, and tRNA are well conserved and structure overlays indicate that both GlnRS proteins conform to a similar 3-dimensional structure. GlnRS was developed into a screening platform using scintillation proximity assay (SPA) technology and used to screen ~2000 chemical compounds. Three inhibitory compounds were identified and analyzed for enzymatic inhibition as well as minimum inhibitory concentrations (MIC) against clinically relevant bacterial strains. Two of the compounds, BM02E04 and BM04H03, were selected for further studies. These compounds displayed broad spectrum anti-bacterial activity and exhibited moderate inhibitory activity against mutant efflux deficient strains of *P. aeruginosa* and *E. coli*. Growth of wild-type strains were unaffected, indicating that efflux was likely responsible for the lack of sensitivity. The global mode of action was determined using time-kill kinetics. BM04H03 did not inhibit growth of human cell cultures at any concentration and BM02E04 only inhibit cultures at the highest concentration tested (400 μ g/ml). In conclusion, GlnRS from *P. aeruginosa* is shown to have a

structure similar to that of *E. coli* GlnRS and two natural product compounds were identified as inhibitors of *P. aeruginosa* GlnRS with the potential for utility as lead candidates in antibacterial drug development in a time of increased antibiotic resistance.

Key words: glutaminyl-tRNA synthetase, protein synthesis, *Pseudomonas aeruginosa*, aminoacyl-tRNA synthetase, drug discovery, antibiotics

INTRODUCTION

In recent years, infectious diseases have become increasingly difficult to treat as a result of resistance to therapeutic remedies by many bacteria. This antibiotic resistance is a major global problem and has attracted a considerable amount of media attention. In a recent report from the Centers for Disease Control and Prevention (CDC), it was estimated that at least 23,000 individuals die each year in the United States from infections caused by pathogens exhibiting resistance to antibiotics.¹ This public health threat can be attributed to several factors, including: misuse as well as overuse of antibacterials in clinical as well as community settings, the tendency of bacteria to acquire resistance due to acquisition of efflux systems, and the low permeability of the bacterial membrane.² Certain bacteria have become resistant to many antibiotics, and these multidrug resistant (MDR) bacteria form a new group of “superbugs” in which there are no known drugs to treat them.³ One pathogen in this group that is of specific concern is *Pseudomonas aeruginosa*, an aerobic, Gram-negative bacteria that is a common cause of healthcare-associated infections including pneumonia, urinary tract infections, and bloodstream infections.⁴ The ability of this bacteria to form resilient biofilms on implanted medical devices such as catheters, as well as on general hospital surfaces and water sources, poses a threat to immunocompromised individuals resulting in higher mortality rates.⁵ Patients with cystic fibrosis (CF) are especially at risk, as *P. aeruginosa* colonizes the lungs of these patients forming biofilms which leads to chronic infections and is a leading cause of death.⁶

The glutamyl tRNA-synthetase (GlnRS), encoded by the *glnS* gene, is an aminoacyl tRNA synthetase (aaRS), which functions by attaching amino acids to cognate tRNAs during protein biosynthesis. GlnRS is a class I tRNA synthetase which is characterized by the presence of two amino acid consensus sequences, HIGH and KMSKS, located in the active site of the catalytic domain formed by the conserved Rossman fold. GlnRS, along with glutamyl-, and arginyl-tRNA synthetases (GluRS and ArgRS) are the only three aaRS requiring the presence of cognate tRNA to form the aminoacyl-adenylate intermediate.⁷ These three tRNA synthetases are further classified as subclass Ib enzymes due to similar subunit structures.⁸

Aminoacylation of a tRNA with the cognate amino acid occurs via a two-step esterification reaction. First, an aminoacyl-adenylate intermediate is formed by the condensation of the amino acid and ATP. Next, the amino acid is transferred to the 2'- or 3'- hydroxyl group of the terminal adenosine of the cognate tRNA.⁹ The attachment of the correct amino acid to its cognate tRNA is vital for the fidelity of protein synthesis. This process is known as tRNA identity but different aaRSs have various different fidelity mechanisms to ensure accuracy.¹⁰ Unlike many other tRNA synthetases, GlnRS has no independent internal editing function to aid in discrimination of near-cognate amino acids such as asparagine or glutamic acid.¹¹ Instead, an induced fit binding mechanism for the binding specificity of glutamine (Gln) by GlnRS is promoted by conformational changes that occur in the active site as a result of binding the anticodon loop of tRNA^{Gln}.¹² In addition, specific nucleotides that are considered to be identity elements in tRNA^{Gln} promote correct tRNA recognition by the cognate synthetase.

The recognition is facilitated by positive elements that allow GlnRS to directly recognize cognate tRNA^{Gln}, and negative elements that block recognition of tRNA^{Gln} by non-cognate synthetases.⁷ In addition to identity elements for binding the correct tRNA, competition by various aaRS proteins for binding cognate tRNAs plays a key role in specificity.¹³ The individual fit mechanism for binding specificity and the specific tRNA^{Gln} identity elements work together to ensure fidelity.

GlnRS is one of only two out of twenty aaRS enzymes which is not found in all organisms, and some prokaryotes lack a tRNA synthetase to attach glutamine to its cognate tRNA^{Gln}. When this is the case, tRNA^{Gln} is mischarged by a non-discriminating (ND) GluRS resulting in Glu-tRNA^{Gln}. The mischarged tRNA^{Gln} is then converted to Gln-tRNA^{Gln} in an amidation reaction by a heterotrimeric amidotransferase (AdT).¹⁴ In *P. aeruginosa*, GluRS is the discriminating type and therefore does not attach a glutamic acid amino acid to tRNA^{Gln}, thus necessitating a functional form of GlnRS.¹⁵

The gene encoding GlnRS from *P. aeruginosa* was cloned and the resulting over-expressed protein was purified and the kinetic parameters (K_M , V_{max} and k_{cat}) governing the interaction with tRNA^{Gln} were determined. The crystal structure of the α_2 form of GlnRS was solved to 1.9 Å resolution. A high-throughput screening platform was then developed and optimized to screen for potential anti-infectives using scintillation proximity assay (SPA) technology. Out of 2000 synthetic and natural chemical compounds, three compounds were identified that inhibited the

activity of *P. aeruginosa* GlnRS. From these three compounds, after scaffold analysis and MIC determination, two were selected for additional characterization.

RESULTS

Protein Expression and Characterization

The glutamyl-tRNA synthetase gene (*glnS*) from *P. aeruginosa* was cloned, expressed and the resulting protein was purified to greater than 98% homogeneity (Fig. S1). The aminoacylation assay described under the “Methods and Materials” section was used to analyze the activity of *P. aeruginosa* GlnRS and to determine the concentrations to be used in downstream assays [Fig. 1(A)]. The aminoacylation reaction occurs via two distinct enzymatic steps. First, binding of ATP and the cognate amino acid allows the formation of an aminoacyl-adenylate. This results from the condensation of the amino acid substrate, in this case glutamine, and ATP, in which ATP is hydrolyzed releasing the β and γ phosphates as PP_i . With all but three of the aaRS enzymes (GluRS, GlnRS and ArgRS), this reaction can occur in the absence of the tRNA and can be monitored using the ATP: PP_i exchange assay to determine the kinetic interaction of the enzyme with either ATP or the amino acid. The results of this assay are indicative of the ability of the enzyme to form an aminoacyl-adenylate in the absence of tRNA followed by reversal of the reaction and subsequent radioactive labeling of ATP in the presence of saturating amounts of [^{32}P] PP_i . In this initial step, formation of an aminoacyl adenylate by GlnRS is “non-productive” in the absence of tRNA^{Gln}, for reasons discussed in the next section. To confirm the requirement for tRNA^{Gln} in the formation of an aminoacyl-adenylate by *P. aeruginosa* GlnRS, the ATP: PP_i exchange assay was monitored in the presence and absence of tRNA [Fig. 1(B)]. In the absence of tRNA^{Gln} [Fig. 1(B), Lane 1] there was no [^{32}P]ATP formed

by the reversal of the condensation reaction. This indicated that no aminoacyl-adenylate had formed. However, in the presence of increasing concentrations of tRNA^{Gln}, increased levels of [³²P]ATP were detected [Fig. 1(B), lane 2-4]. This indicated that in the presence of tRNA an aminoacyl-adenylate was formed. However, the low level of radioactive ATP formed suggests that the reversal of the reaction is not a dynamic process, likely because the reaction goes to fulfillment and the tRNA is aminoacylated.

Next, the kinetic interactions of *P. aeruginosa* GlnRS with its cognate tRNA substrate were determined using the aminoacylation assay. The initial rate for aminoacylation was determined at several concentrations of tRNA^{Gln} (0.5-2 μM) while holding the concentrations of ATP and Gln constant at 2.5 mM and 100 μM, respectively [Fig. 1(C)]. The initial velocities were modeled by fitting them to the Michaelis-Menten steady-state model using XLfit (IDBS). The K_M and the observed enzyme turn-over values (k_{cat}^{obs}) were determined to be 1.0 μM and 0.15 s⁻¹ for *P. aeruginosa* GlnRS, which gave a k_{cat}^{obs}/K_M value of 0.15 s⁻¹μM⁻¹. The same values determined for *Escherichia coli* GlnRS were 0.15 μM, 0.2 s⁻¹, and 0.95 s⁻¹μM⁻¹, respectively.¹⁶ The minor variation in the K_M values could be a result of the codon usage or tRNA^{Gln} isotype concentration variation found in *P. aeruginosa* relative to that in *E. coli*.

Structure and Sequence Analysis

P. aeruginosa GlnRS incubated with MgCl₂ and AMPPNP crystallized into space group *P2* and crystals diffracted to 1.9 Å resolution with a single homodimer in the asymmetric unit [Fig.

2(A)] (PDB ID: 5BNZ). Despite the presence of MgCl₂ and AMPPNP in the crystallization conditions and AMPPNP and L-glutamine in the soaking conditions, no evidence of any ligand was observed in the electron density. Data collection and refinement statistics are given in Table I. *P. aeruginosa* GlnRS formed a typical GlnRS structure containing five distinct domains: dinucleotide fold domain (DNF), acceptor stem binding domain (ABD), helical sub-domain, proximal beta-barrel, and distal beta-barrel [Fig. 2(B)].

The structure of *E. coli* GlnRS with ATP and tRNA^{Gln} (PDB ID: 1GSG), with a glutaminyladenylate analog and tRNA^{Gln} (PDB ID: 1QTQ) or without any ligands (PDB ID: 1NYL) have been well studied, primarily from the 3-dimensional structures of GlnRS from *E. coli*.¹⁷⁻¹⁹ More recently, the structure of GlnRS from *Deinococcus radiodurans* has been solved.²⁰ This protein, albeit similar to the *E. coli* GlnRS, contains a unique C-terminal Yqey domain and will not be discussed here. A comparison of the amino acid primary structure of *E. coli* and *P. aeruginosa* GlnRS reveals a high degree of sequence conservation and the residues that come in direct contact with ATP, glutamine, and tRNA^{Gln} are highly conserved (Fig. 3). This is consistent with alignment studies where a high level of sequence conservation was observed (average 68/56% similar/identical residues) when GlnRS was compared with 33 GlnRS proteins across the eubacterial phylum (Table S1). Interestingly, the greatest variation occurred when the amino acid sequence of *P. aeruginosa* GlnRS was compared with that of GlnRS from the epsilonproteobacteria phyla, in which there was only 47.3/38.6 similar/identical residues. The

high level of sequence conservation indicates that recognition of the substrates and insurance of specificity in substrate selection likely occurs in a similar fashion in these enzymes.

The DNF domain contains the catalytic active site of GlnRS and it is composed of two sections separated by the ABD domain. The first half contains the signature HIGH motif, while the KMSKS motif is contained within the second half of the DNF domain (Fig. 3). This active site region contains binding sites for ATP and glutamine as well as the acceptor stem of tRNA^{Gln}. The amino acids observed to form contacts with these substrates in the DNF of *E. coli* GlnRS are almost strictly conserved in the *P. aeruginosa* GlnRS (Fig. 4). During the process of substrate binding, certain amino acid residues in the ABD make contact with the acceptor stem, guiding it through conformational rearrangements to the active site in the DNF domain.¹² There is a high degree of sequence conservation seen in the alignment in Figure 3, and the residues contacting the acceptor stem of the tRNA in *E. coli* GlnRS are conserved or similar in the *P. aeruginosa* enzyme.

The mechanism of identification of the cognate amino acid and discrimination of non-cognate amino acids allows the aminoacyl tRNA synthetases to be divided into two groups. The aaRS enzymes in the first group have a proofreading function in the form of an editing domain that ensures cognate acylation of tRNA. The editing occurs either at the pre-transfer state, in which the mis-activated amino acid-adenylate is hydrolyzed before attachment to the 3'-end of the cognate tRNA, or at the post-transfer state, in which the non-cognate amino acid of the mischarged tRNA is hydrolyzed.²¹ The other group of aaRS enzymes ensure cognate acylation

of tRNA by a process other than editing. In the case of *E. coli*, GlnRS binds ATP and glutamine as a result of structural rearrangements in the active site induced by cognate tRNA binding.¹⁷

This precludes the binding of other potential amino acid substrates besides glutamine and glutamic acid. To distinguish between glutamine and glutamic acid, two residues in the active site are essential (Fig. 4): Arg30 (*E. coli* numbering) recognizes the carbonyl carbon of glutamine through electrostatic interactions, and Tyr211 acts as a “negative determinant” against binding of glutamic acid by potentially forming hydrogen bonds with the two amide hydrogens of glutamine, thereby stabilizing binding.^{11,18} These residues are strictly conserved between *E. coli* and *P. aeruginosa* GlnRS.

The anticodon of the tRNA is a major determinate for selection of the cognate tRNA, and the two carboxyl-terminal domains of GlnRS make contacts with this region of the tRNA, acting to discriminate in favor of binding tRNA^{Gln} out of the pool of tRNAs.¹⁹ The three nucleotides composing the anticodon interact with specific amino acid residues. First, there are two isoacceptors for tRNA^{Gln} (CUG and UUG). The pocket for binding either U34 or C34 accommodates either of the pyrimidines, but discriminates against a purine.²² Within the pocket U34/C34 appears to form hydrogen bonds with Arg410/Arg412 (*P. aeruginosa/E. coli*), allowing a certain amount of wobble room. Next, U35 has a tight binding pocket and movement is limited by interactions with a number of amino acid residues. Arg412, Lys401, and Arg520 (*E. coli* numbering) stabilize U35 through ionic interactions with the two adjacent phosphates. Arg520 also packs against one side of U35 and forms a hydrogen bond with the 2-keto of the uracil base.

Pro369 packs against the other side of U35, holding it rigidly in place. Arg341, Gln517, and Glu519 recognize U35 by forming hydrogen bonds with the 4-keto group, N3, and the 2-keto group, respectively, of the uracil ring. Finally, G36 fits into a pocket specific for the guanosine, which is recognized by hydrogen bonding of the guanidinium group of Arg402 to N7 and the 6-keto group of guanine.²² All of these amino acid residues making contact with the anticodon are strictly conserved in GlnRS from both *E. coli* and *P. aeruginosa* (Fig. 5) indicating a similar mechanism of action.

Screening for Inhibitors of P. aeruginosa GlnRS Activity

Using SPA technology, the activity of GlnRS in the aminoacylation assay was screened against three chemical compound libraries to identify inhibitory compounds. First, a collection of 320 natural products, mostly derived from plants, was from the Prestwick Phytochemical Library. The second was the NatProd Collection from Microsource Discovery Systems, composed of 800 natural products, including simple and complex oxygen heterocycles, alkaloids, sesquiterpenes, diterpenes, pentacyclic triterpenes, and sterols. Finally, the Anti-infective Library from TimTec, LLC contained 890 low molecular weight synthetic compounds with scaffolds based on known anti-bacterial, anti-fungal, and anti-microbial agents. The assay detects the ability of GlnRS to aminoacylate tRNA^{Gln} and to measure the effect of a chemical compound on the aminoacylation activity. Chemical compounds were dissolved in 100% dimethyl sulfoxide (DMSO) resulting in final DMSO concentrations of 4% in the screening

assays. To determine the effect on the enzymatic activity, DMSO was added to the aminoacylation assay at increasing amounts. There was no decrease of activity observed in the aminoacylation assays containing up to 7% DMSO and only a moderate decrease in activity to 10% DMSO [Fig. 6(A)]. Next, tRNA was titrated into the assay to determine the concentration of tRNA^{Gln} to be used in the screening assay with the goal of insuring that the amount of tRNA^{Gln} used would be within the linear region of the reaction-detection time [Fig. 6(B)]. From the titration reactions, ~1 μM tRNA^{Gln} was selected for use in the screening assays. The other components of the assay were also optimized for maximum activity (Fig. S2). The chemical compound concentration in the initial screening assays was 132 μM and screening was carried out as single point assays. Compounds observed to inhibit at least 50% of enzymatic activity were re-assayed in triplicate. These assays resulted in three confirmed hit compounds, BM02E04, BM04B05, and BM04H03, all from the natural product library (Fig. 7). Initially, the potency of the compounds for inhibiting the enzymatic activity of GlnRS was determined (Fig. 8). To do this, the compounds were titrated into aminoacylation assays, resulting in concentrations of compound ranging from 200 μM to 0.4 μM . The IC₅₀ values for BM02E04, BM04B05, and BM04H03 were determined to be 1.9, 2.5, and 40 μM , respectively.

Microbiological Assays

The three hit compounds were tested in broth microdilution assays to determine minimum inhibitory concentrations (MIC) against a panel of 10 pathogenic bacteria, including efflux pump mutants of *E. coli* and *P. aeruginosa* and a hypersensitive strain of *P. aeruginosa* (Table S2). Quality control of test antibiotics was monitored by testing against the same panel of bacteria (Table S3). BM02E04 inhibited the growth of all Gram-positive organisms: *Staphylococcus aureus* and *Streptococcus pneumoniae* at 64 µg/ml and *Enterococcus faecalis* at 4 µg/ml. BM04H03 inhibited growth of *E. faecalis*, *S. aureus* and *S. pneumoniae* with MIC values of 64, 8, and 64 µg/ml. These two compounds, BM02E04 and BM04H03, had good MICs against the Gram-negative *Moraxella catarrhalis* (32 and 0.125 µg/ml, respectively). Interestingly, cultures of the respiratory pathogen, *Haemophilus influenzae*, were only slightly affected by the compounds. BM02E04 exhibited a modest MIC against the mutant form of *E. coli* (*E. coli tolC*), while BM04H03 showed a significant decrease in the MIC value against the efflux deficient strain. When compared with the lack of inhibition of the wild-type strain, this indicated that efflux was a likely mechanism for the lack of sensitivity. Both compounds were also observed to have a low level of activity against *P. aeruginosa* PA200, the efflux pump mutant, and the hypersensitive strain, again indicating that the lack of sensitivity of the wild-type *P. aeruginosa* may be due to efflux. There was no activity observed against the wild-type strains of either *E. coli* or *P. aeruginosa* at concentrations below 128 µg/ml. Based on compound scaffold analysis

and broad spectrum activity against both Gram-positive and Gram-negative pathogens, two of the compounds, BM02E04 and BM04H03 were selected for further analysis.

Next, time kill kinetic studies were performed to determine the global mode of inhibition of bacterial growth in cultures. Based on MIC results, both compounds were tested against cultures of the Gram-positive bacteria, *S. aureus*, and the Gram-negative *M. catarrhalis*. All cultures contained compounds at four times the MIC and samples were analyzed between 0 and 24 hours [Fig. 9(A), 9(B)]. Both BM02E04 and BM04H03 were observed to inhibit *S. aureus* with a bacteriostatic global mode of inhibition. They displayed constant growth but a decrease in colony forming units (CFU) of 2 to 6 log₁₀ compared to the control during the initial six hours. BM04H03 was also observed to inhibit growth of the Gram-negative *M. catarrhalis*, with a bacteriostatic mode of inhibition. However, BM02E04 was bactericidal when tested against *M. catarrhalis* and inhibited bacterial growth by killing the bacteria.

MTT assays were performed to examine whether the hit compounds BM02E04 and BM04H03 were cytotoxic to human cells, and if they were toxic, to determine the concentration at which growth was inhibited by 50% (CC₅₀). Human embryonic kidney 293 (HEK293) cells were treated with concentrations of each compound separately at 25-400 µg/ml for 24 hours under standard tissue culture conditions in triplicate. There was only a slight decrease in cell viability in the presence of BM02E04 at the highest concentration tested (400 µg/ml) and BM04H03 was not observed to be toxic to cells at any concentration tested [Fig. 9(C), 9(D)]. The low level of toxicity observed in these early tests is advantageous in development of

potential antimicrobial agents and indicates that both compounds may be amenable to further development as therapeutics.

DISCUSSION

The aminoacyl-tRNA synthetases are essential components of protein synthesis and are vital for cell growth in all organisms. In the quest for discovery of new and different agents with which to fight bacterial infections, it is important that the molecular targets upon which these agents act be sufficiently distinct when compared with the eukaryotic homolog. The group of aaRS enzymes from bacterial origins as a whole are divergent in amino acid primary structure compared with that of eukaryotic counterparts. This difference makes them good targets for development of new antibacterial agents. When *P. aeruginosa* GlnRS was compared with the human cytosolic form of GlnRS (hGlnRS), there was only 40.6/31.8% similar/identical amino acids observed. However, this is a bit misleading since the hGlnRS contains an N-terminal 200 amino acid domain that functions in the formation of a multi-synthetase complex that is not part of the bacterial GlnRS.²³ When this domain was removed from the amino acid sequence of hGlnRS and the truncated polypeptide was compared with the full amino acid sequence of *P. aeruginosa* GlnRS, the percentage of similar/identical residues increased to 57.5/45.0, respectively. This degree of amino acid sequence similarity observed between human and *P. aeruginosa* GlnRS is higher than the similarity between eukaryotic and prokaryotic aaRS enzymes in general. However, when BM02E04 and BM04H03 were tested in human cell

cultures, there was almost a complete absence of toxicity, indicating these compounds did not target the human enzyme and do have good potential for development as therapeutic agents. The amino acid sequence of *P. aeruginosa* GlnRS, when compared to homologs from other members of the eubacteria phyla contained ~68/56% similar/identical sequence conservation. This increased level of sequence conservation may argue for broad spectrum activity against various bacteria, which is also supported by the finding in MIC testing that these compounds were observed to be active against both Gram-negative and Gram-positive pathogens.

We show here the three-dimensional crystal structure for *P. aeruginosa* GlnRS solved to 1.9 Å, which allows identification and comparison of regions critical for enzymatic function relative to the well-studied *E. coli* enzyme. The structure of *E. coli* GlnRS was previously solved bound to each of the three substrates (ATP, glutamine, and tRNA^{Gln}) which allows us to directly compare essential amino acid residues making contact with the substrates. In this comparison, we found that the critical amino acid residues were structurally conserved, indicating likely conservation of function as well as structure.

Scintillation proximity assay technology was used to develop a screen for inhibitors of the activity of *P. aeruginosa* GlnRS. The screening assays were robust and resulted in Z' and Z factors of approximately 0.55 and 0.33, respectively, across all plates. The signal to background ratio of the unaffected enzyme activity to the EDTA controls was approximately 6:1. From over 2000 compounds, 5 compounds from the TimTec LLC compound library and 15 from the MicroSource Discovery Systems were identified that inhibited the activity of *P. aeruginosa*

GlnRS. After removing compounds that had activity against multiple aaRS enzymes from *P. aeruginosa*, three compounds, BM02E04, BM04B05, and BM04H03, were chosen for additional analysis. All three compounds exhibited inhibition of enzymatic activity. However, structure analysis and the lack of activity against bacteria in culture resulted in the removal of BM04B05 from further consideration. BM02E04 and BM04H03 exhibited moderate MICs against Gram-positive bacteria as well as against efflux mutant forms of *E. coli* and *P. aeruginosa*. Time-kill studies indicated that these two compounds were bacteriostatic against cultures of *S. aureus*. This would be the expected mode of action for compounds that inhibit the activity of an aaRS, since inhibition of the aminoacylation activity mimics starvation for amino acids by lowering the ratio of charged to uncharged tRNA, and induces the stringent response resulting in static bacterial growth. BM04H03 was also bacteriostatic against cultures of the Gram-negative *M. catarrhalis*. However, BM02E04 displayed a bactericidal mode of inhibition in these bacterial cultures. The bactericidal form of inhibition observed with BM02E04 may be due to inhibition of secondary roles and functions as well as inhibition of the aminoacylation function. Many secondary roles have been observed for members of the aaRS group of enzymes.²⁴

A search of PubChem identified BM02E04 as purpurogallin-4-carboxylic acid (CID: 269315). There is little data on the bioactivity of this compound, but it has been shown to be active as an anti-oxidant and in PubChem bioassays (AID:1259374) to decrease the activity of human microphthalmia-associated transcription factor. The core scaffold (purpurogallin) is a natural phenol, and has shown activity in numerous PubChem bioassays.

BM04H03 was identified in PubChem as cryptotanshinone (CID: 160254).

Cryptotanshinone, a diterpene quinone, is isolated from the roots of the plant *Salvia miltiorrhiza Bunge* and has been widely used in traditional Chinese medicine for treatment of a variety of diseases. Recently, cryptotanshinone has been shown to have anti-cancer activity.²⁵ The finding that these natural product compounds are bio-active in a number of assays, may reduce the potential for development as an antibacterial, since this may increase the likelihood of toxicity. However, cryptotanshinone has been shown to be well tolerated in numerous clinical settings.

As noted above, both BM02E04 and BM04H03 were observed to have moderate MIC values against the three Gram-positive bacteria, *E. faecalis*, *S. aureus*, and *S. pneumoniae*. This is an interesting observation since these three organisms do not contain a GlnRS enzyme, instead they contain a non-discriminating (ND) GluRS, which charges both tRNA^{Glu} and tRNA^{Gln} with glutamic acid. The ND-GluRS from these three Gram-positive bacteria as well as GlnRS from numerous other eubacteria (see Table S1) must all recognize tRNA^{Gln} as a cognate tRNA. When we carried out BLAST searches against the *E. faecalis*, *S. aureus*, and *S. pneumoniae* databases using the *P. aeruginosa* GlnRS amino acid sequence as the query sequence, the ND-GluRS proteins were the primary hits. The “sequences producing significant alignments” portion of the various ND-GluRS proteins in the BLAST results ranged from 303 amino acid residues to the full length proteins, and in the alignments with the corresponding amino acid sequence of GlnRS from *P. aeruginosa* revealed a high degree of conservation. In particular, we aligned the overall amino acid sequence of GlnRS from *P. aeruginosa* with that of the ND-GluRS from *S.*

pneumoniae (accession VTQ31436), the results indicated a similar conservation of amino acids (71/60 %, similar/identical) as observed when the sequence of *P. aeruginosa* GlnRS was compared with the amino acid sequence of GlnRS from other eubacteria (Table S1). It is an intriguing possibility that inhibition by these compounds of the growth of these bacteria in culture may be the result of inhibition of the ND-GluRS proteins. Further work will be necessary to determine whether BM02E04 and BM04H03 also target the ND-GluRS proteins of these bacteria.

METHODS AND MATERIALS

Materials

All chemicals were obtained from Fisher Scientific (Pittsburg, PA). DNA oligonucleotides were from Integrated DNA Technologies (Coralville, IA). DNA sequencing was performed by Functional Bioscience (Madison, WI). Radioactive isotopes, SPA beads and 96-well screening plates were from PerkinElmer (Waltham, MA). The natural compound libraries were from MicroSource Discovery Systems (Gaylordsville, CT) and Prestwick Chemical, Inc. (Strasbourg-Illkirch, France), and the synthetic compound library was from TimTec LLC (Newark, DE). Compounds stocks were dissolved in dimethyl sulfoxide (DMSO) to a concentration of 10 mM, stored at -20°C and thawed immediately before analysis. The compounds had an average purity of 95%, and the minimum purity is at least 90%.

Cloning and Purification

Polymerase chain reaction (PCR) was used to amplify the gene encoding *P. aeruginosa* GlnRS (MJ Mini Thermo Cycler, Bio-Rad, Hercules, CA) using *P. aeruginosa* PAO1 (ATCC 47085) genomic DNA as a template. An *NheI* restriction site was added at the 5' end of the gene using a forward primer (5'-CCAAGCTAGCAAGCCAGAGACCACC-3') and a *HindIII* restriction site was added at the 3' end using a reverse primer (5'-CAACAAGCTTTCAGCCCTGTCCCCAG-3'). The amplified gene was inserted into the pET-28b(+) plasmid (Novagen) digested with *NheI* and *HindIII* restriction enzymes. This recombinant plasmid was transformed into *E. coli* Rosetta 2 (DE3) Singles Competent Cells (EMD Millipore, Danvers, MA).

Bacterial cultures were grown in Terrific Broth (TB) containing 25 µg/mL of kanamycin and 50 µg/mL of chloramphenicol at 37°C. At an optical density (A_{600}) of 0.6 the overexpression of *P. aeruginosa* GlnRS was induced by addition of isopropyl β-D-1-thiogalactopyranoside (IPTG) to a concentration of 0.5 mM. The culture was grown for 4 hours post-induction and bacteria were harvested by centrifugation (10,000 g, 4°C, 45 min). Fraction I lysates were prepared²⁶ and purification of *P. aeruginosa* GlnRS was initiated by addition of ammonium sulfate (AS) to 60% saturation resulting in precipitation of the target enzyme. *P. aeruginosa* GlnRS was further purified using nickel-nitrilotriacetic acid (Ni-NTA) affinity chromatography (Perfect Pro, 5 Prime)²⁷ and then dialyzed twice against a buffer (2L) containing: 20 mM HEPES-KOH (pH 7.0), 40 mM KCl, 1 mM MgCl₂, 0.1 mM EDTA, and 10% glycerol. Purified protein were aliquoted and flash frozen in liquid nitrogen.

Gel Electrophoresis and Protein Assays

For sodium dodecyl sulfate-polyacrylamide gel electrophoresis (SDS-PAGE), 4-12% polyacrylamide precast gradient gels (Novex NuPAGE; Invitrogen) were used with 3-(N-morpholino)propanesulfonic acid (MOPS) as the running buffer (Invitrogen). The gels were stained with Simply Blue Safe Stain (Invitrogen) to visualize the proteins. The protein standard was the EZ-Run Rec Ladder (Fisher Scientific). Coomassie Protein Assay Reagent (Thermo Scientific, Waltham, MA) was used to determine protein concentrations with bovine serum albumin as a standard.

ATP:PP_i Exchange Reactions

ATP:PP_i exchange reactions (100 μ L) were carried out at 37°C for 20 min in 50 mM Tris-HCl (pH 7.5), 10 mM KF, 8 mM MgOAc, 1 mM dithiothreitol (DTT), 2 mM [³²P]PP_i (50 cpm/pmol), 2 mM ATP, 2 mM glutamine and 0.2 μ M of *P. aeruginosa* GlnRS as described.¹⁵ The reactions were carried out in the absence and in the presence of tRNA^{Gln} (0.3, 0.6, 1.2 μ M).

Timed tRNA Aminoacylation Assay

Aminoacylation reactions were used to determine initial velocities at various concentrations of tRNA^{Gln}. These reactions were carried out at 37°C and stopped at time intervals ranging from 1 to 5 minutes. Reactions (50 μ L) contained a component mixture to yield final concentrations of 50 mM Tris-HCl (pH 7.5), 5 mM MgCl₂, 2.5 mM ATP, 1 mM DTT, 75 μ M [³H]Gln (50

cpm/pmol), and 0.025 μM *P. aeruginosa* GlnRS. Reactions were initiated by addition of tRNA^{Gln} at varied concentrations (0.5 to 2.0 μM). Reactions were stopped by the addition of 2 ml of 5% (v/v) ice-cold trichloroacetic acid (TCA), placed on ice for 10 min, and then filtered through glass fiber filters (Millipore, type HA 0.45 mm). Filters were washed with 10 mL ice-cold 5% TCA and dried. The filters were analyzed using an LS6500 multi-purpose scintillation counter (Beckman Coulter). Initial velocities for aminoacylation were calculated for all tRNA concentrations. Data were fit to the Michaelis-Menten steady-state model to determine the K_M and V_{max} values.

Crystallography and Structure Determination

P. aeruginosa GlnRS was cloned, expressed, and purified for crystallography as described.²⁸ In preparation for crystallography, the GlnRS protein was concentrated to 20.0 mg/ml (SSGCID batch ID PsaeA.18222.aB1.PW37623), and incubated with 2.5 mM MgCl_2 and 2.5 mM AMPPNP for 10 min at 290 K. Crystals were then grown at 290 K by sitting drop vapor diffusion with 0.4 μl of protein/ligand complex mixed with 0.4 μl of a condition based on Microlytic MCSG1, well c2:23% (w/v)PET-3350, 0.2 M lithium sulfate, and 0.1 M Bis-Tris:HCl (pH 6.5). Crystals were looped and soaked in reservoir solution supplemented with 20% ethylene glycol, 2.5 mM L-glutamine, 2.5 mM MgCl_2 , and 2.5 mM AMPPNP and flash frozen in liquid nitrogen. Data were collected at 100 K on a Rayonix MX-225 mm CCD detector at a wavelength of 0.97872 Å on beamline 21-ID-F at Life Sciences Collaborative Access Team (LS-

CAT) at the Advanced Photon Source (APS, Argonne, IL, USA). Data were reduced with the XDS/XSCALE package (REF).²⁹ The structure was solved using molecular replacement with BALBES³⁰ and 1NYL as a starting model. Iterative rounds of manual model building and automated refinement were carried out using Coot³¹ and Phenix.³² The structure was quality checked with Molprobit.³³

Chemical Compound Screening

The tRNA aminoacylation assay was developed into a screening platform for identification of inhibitory compounds using scintillation proximity assay (SPA) technology. Screening reactions were carried out in 96-well microtiter plates. Test compounds, dissolved in 100% DMSO (2 μ L of compound; 3.3 mM), were equilibrated by addition of 33 μ L of the component mixture described above and incubated at ambient temperature for 15 min. Control reactions contained DMSO in the absence of compound. Other control assays to yield an assay baseline were carried out in the presence of 50 μ M ethylenediaminetetraacetic acid (EDTA). The concentration of *P. aeruginosa* GlnRS was 0.12 μ M. Reactions were initiated by the addition of 15 μ L *E. coli* tRNA (~1.0 μ M tRNA^{Gln}) and incubated for 1 h at 37°C. Reactions were stopped by the addition of 5 μ L of 0.5 M EDTA. 400 μ g of yttrium silicate (Ysi) poly-L-lysine coated SPA beads (Perkin-Elmer) in 150 μ L of 300 mM citric acid were added to the reaction and allowed to incubate at room temperature for 1 h. Reactions were analyzed using a 1450 Microbeta (Jet) liquid scintillation/luminescent counter (Wallac). Assays to determine IC₅₀

values were performed with the test compounds serially diluted from 200 μM to 0.4 μM . The IC_{50} was determined by fitting the data to a Sigmoidal Dose-Response Model using XLfit (IDBS).

Microbiological Assays

Broth microdilution minimum inhibitory concentration (MIC) testing was carried out according to Clinical Laboratory Standards Institute guidelines M7-A7.³⁴ MIC values were determined against a panel of bacteria which included: *E. coli* (ATCC[®] 25922), *E. coli TolC mutant*, *Enterococcus faecalis* (ATCC[®] 29212), *Haemophilus influenzae* (ATCC[®] 49766), *Moraxella catarrhalis* (ATCC[®] 25238), *P. aeruginosa* (ATCC[®] 47085), *P. aeruginosa* PAO200 (efflux pump mutant), *P. aeruginosa hypersensitive strain* (ATCC[®] 35151), *Staphylococcus aureus* (ATCC[®] 29213), and *Streptococcus pneumoniae* (ATCC[®] 49619).

Time-kill studies were performed using *M. catarrhalis* and *S. aureus* based on the MIC assay results, according to CLSI document M26-A.³⁵ Growth media was Brain Heart Infusion and Trypticase Soy Broth from Remel (Lenexa, KS). The compound concentration was four times the MIC.

In Vitro Cytotoxicity Test

The toxic effect of each compound on the growth of human cell cultures was determined as described using human embryonic kidney 293 cells (HEK-293).¹⁵ MTT assays were carried out

in triplicate at each compound concentration (25 µg/ml to 400 µg/ml). Student's two-tiered T-test was utilized to assess statistical significance.

Supplemental Material

- Supplemental Figure S1. Purification of *P. aeruginosa* GlnRS.
- Supplemental Figure S2. Titration of non-enzymatic components into the aminoacylation assay for determination of the concentration to be used in the screening assays.
- Supplemental Table 1. Comparison of the amino acid sequence of *P. aeruginosa* GlnRS with the homolog from various other eubacteria.
- Supplemental Table 2. MIC values of the hit compounds observed to inhibit the activity of *P. aeruginosa* GlnRS.
- Supplemental Table 3. The MIC of control antibiotics against the panel of pathogenic bacteria were tested for quality control.

Acknowledgements

The authors are grateful for the financial support provided by the National Institutes of Health (grant number: 1SC3GM098173). The contents of this article are solely the responsibility of the authors and do not necessarily represent the official views of the National Institutes of Health. A portion of graduate student support was from a departmental grant from the Robert A. Welch Foundation (Grant No. BG-0017). Partial undergraduate support was from an NIH

UTRGV RISE program, grant # 1R25GM100866. Structural work for this project was funded in part by the National Institute of Allergy and Infectious Diseases, National Institutes of Health, Department of Health and Human Services, under Contract No.: HHSN272201700059C. This research used resources of the Advanced Photon Source, a U.S. Department of Energy (DOE) Office of Science User Facility operated for the DOE Office of Science by Argonne National Laboratory under Contract NO. DE-AC02-06CH11357. Use of the LS-CAT Sector 21 was supported by the Michigan Economic Development Corporation and the Michigan Technology Tri-Corridor (Grant 085P1000817).

Declaration of Conflicting Interests

The authors declared no potential conflicts of interest with respect to the research, authorship, and/or publication of this article.

References

1. CDC (2013) Antibiotic Resistance in the United States, 2013.
<https://www.cdc.gov/drugresistance/biggest-threats.html>
2. Ventola CL (2015) The antibiotic resistance crisis: part 1: causes and threats. *P T* 40:277-283.
3. Poole K (2011) *Pseudomonas aeruginosa*: resistance to the max. *Front Microbiol* 2:65.
4. Nathwani D, Raman G, Sulham K, Gavaghan M, Menon V (2014) Clinical and economic consequences of hospital-acquired resistant and multidrug-resistant *Pseudomonas aeruginosa* infections: a systematic review and meta-analysis. *Antimicrob Resist Infect Control* 3:32
5. Mulcahy LR, Isabella VM, Lewis K (2014) *Pseudomonas aeruginosa* biofilms in disease. *Microb Ecol* 68:1-12.
6. Palmer GC, Whiteley M (2015) Metabolism and pathogenicity of *Pseudomonas aeruginosa* infections in the lungs of individuals with cystic fibrosis. *Microbiol Spectr* 3:MBP-0003-2014.
7. Rogers MJ, Weygand-Durasevic I, Schwob E, Sherman JM, Rogers KC, Adachi T, Inokuchi H, Soll D (1993) Selectivity and specificity in the recognition of tRNA by *E. coli* glutaminyl-tRNA synthetase. *Biochimie* 75:1083-1090.
8. Bullwinkle TJ, Ibba M (2014) Emergence and evolution. *Top Curr Chem* 344:43-87.

9. Tan M, Wang M, Zhou XL, Yan W, Eriani G, Wang ED (2013) The Yin and Yang of tRNA: proper binding of acceptor end determines the catalytic balance of editing and aminoacylation. *Nucleic Acids Res* 41:5513-5523.
10. Martinis SA, Boniecki MT (2010) The balance between pre- and post-transfer editing in tRNA synthetases. *FEBS Lett* 584:455-459.
11. Bullock TL, Uter N, Nissan TA, Perona JJ (2003) Amino acid discrimination by a class I aminoacyl-tRNA synthetase specified by negative determinants. *J Mol Biol* 328:395-408.
12. Uter NT, Perona JJ (2006) Active-site assembly in glutaminyl-tRNA synthetase by tRNA-mediated induced fit. *Biochemistry* 45:6858-6865.
13. Sherman JM, Rogers MJ, Soll D (1992) Competition of aminoacyl-tRNA synthetases for tRNA ensures the accuracy of aminoacylation. *Nucleic Acids Res* 20:2847-2852.
14. Akochy PM, Bernard D, Roy PH, Lapointe J (2004) Direct glutaminyl-tRNA biosynthesis and indirect asparaginyl-tRNA biosynthesis in *Pseudomonas aeruginosa* PAO1. *J Bacteriol* 186:767-776.
15. Hu Y, Guerrero E, Keniry M, Manrique J, Bullard JM (2015) Identification of chemical compounds that inhibit the function of glutamyl-tRNA synthetase from *Pseudomonas aeruginosa*. *J Biomol Screen* 20:1160-1170.
16. Jahn M, Rogers MJ, Soll D (1991) Anticodon and acceptor stem nucleotides in tRNA(Gln) are major recognition elements for *E. coli* glutaminyl-tRNA synthetase. *Nature* 352:258-260.

17. Sherlin LD, Perona JJ (2003) tRNA-dependent active site assembly in a class I aminoacyl-tRNA synthetase. *Structure* 11:591-603.
18. Rath VL, Silvian LF, Beijer B, Sproat BS, Steitz TA (1998) How glutamyl-tRNA synthetase selects glutamine. *Structure* 6:439-449.
19. Rould MA, Perona JJ, Soll D, Steitz TA (1989) Structure of *E. coli* glutamyl-tRNA synthetase complexed with tRNA(Gln) and ATP at 2.8 Å resolution. *Science* 246:1135-1142.
20. Deniziak M, Sauter C, Becker HD, Paulus CA, Giege R, Kern D (2007) *Deinococcus* glutamyl-tRNA synthetase is a chimera between proteins from an ancient and the modern pathways of aminoacyl-tRNA formation. *Nucleic Acids Res* 35:1421-1431.
21. Beuning PJ, Musier-Forsyth K (2000) Hydrolytic editing by a class II aminoacyl-tRNA synthetase. *Proc Natl Acad Sci USA* 97:8916-8920.
22. Rould MA, Perona JJ, Steitz TA (1991) Structural basis of anticodon loop recognition by glutamyl-tRNA synthetase. *Nature* 352:213-218.
23. Ognjenovic J, Wu J, Matthies D, Baxa U, Subramaniam S, Ling J, Simonovic M (2016) The crystal structure of human GlnRS provides basis for the development of neurological disorders. *Nucleic Acids Res* 44:3420-3431.
24. Martinis SA, Plateau P, Cavarelli J, Florentz C (1999) Aminoacyl-tRNA synthetases: a family of expanding functions. *EMBO J* 18:4591-4596.

25. Chen W, Lu Y, Chen G, Huang S (2013) Molecular evidence of cryptotanshinone for treatment and prevention of human cancer. *Anticancer Agents Med Chem* 13:979-987.
26. Cull MG, McHenry CS (1995) Purification of *Escherichia coli* DNA polymerase III holoenzyme. *Methods Enzymol* 262:22-35.
27. Palmer SO, Rangel EY, Hu Y, Tran AT, Bullard JM (2013) Two homologous EF-G proteins from *Pseudomonas aeruginosa* exhibit distinct functions. *PLoS One* 8:e80252.
28. Bryan CM, Bhandari J, Napuli AJ, Leibly DJ, Choi R, Kelley A, Van Voorhis WC, Edwards TE, Stewart LJ (2011) High-throughput protein production and purification at the Seattle Structural Genomics Center for Infectious Disease. *Acta Cryst F* 67:1010-1014.
29. Kabsch W (2010) Integration, scaling, space-group assignment and post-refinement. *Acta Cryst D* 66:133-144.
30. Long F, Vagin AA, Young P, Murshudov GN (2008) BALBES: a molecular-replacement pipeline. *Acta Cryst D* 64:125-132.
31. Emsley P, Cowtan K (2004) Coot: model-building tools for molecular graphics. *Acta Cryst D* 60:2126-2132.
32. Adams PD, Afonine PV, Bunkoczi G, Chen VB, Davis IW, Echols N, Headd JJ, Hung LW, Kapral GJ, Grosse-Kunstleve RW, McCoy AJ, Moriarty NW, Oeffner R, Read RJ, Richardson DC, Richardson JS, Terwilliger TC, Zwart PH (2010) PHENIX: a

- comprehensive Python-based system for macromolecular structure solution. *Acta Cryst D66*:213-221.
33. Chen VB, Arendall WB III, Headd JJ, Keedy DA, Immormino RM, Kapral GJ, Murray LW, Richardson JS, Richardson DC (2010) MolProbity: all-atom structure validation for macromolecular crystallography. *Acta Cryst D66*:12-21.
 34. Methods for Dilution Antimicrobial Susceptibility Test for Bacteria that Grow Aerobically: Approved Guidelines M7-A7. CLSI, Wayne PA. M7-A7. 2006. Clinical and Laboratory Standards Institute.
 35. Methods for Determining Bactericidal Activity of Antimicrobial Agents: Approved Guideline M26-A. CLSI, Wayne, PA. M26-A. 2002. Clinical and Laboratory Standards Institute.

Table 1Data collection and refinement statistics for the crystal structure of *P. aeruginosa* GlnRS.

Data collection	
PDB code	5BNZ
Resolution (Å)	50-1.90 (1.95-1.90)
Space Group	<i>P2</i>
Unit Cell Dimensions	
• a, b, c (Å)	109.01 56.02 127.14 187.24
• α, β, γ , (°)	90.00, 99.41, 90.00
No. of unique reflections	119747
R_{merge}	9.5 (46.1)
Redundancy	5.0 (5.0)
Completeness (%)	99.8 (99.6)
I/σ	11.71 (3.31)
$CC_{1/2}$	99.7 (83.9)
Refinement	
Resolution (Å)	1.90 (1.95-1.90)
No. of protein atoms	8743
No. of sulfate atoms	20
No. of Cl atoms	2
No. of water molecules	1522
R_{working} (R_{free})	18.8 (22.8)
R.M.S. deviations	
• Bond lengths (Å)	0.007
• Bond angles (°)	1.006
Ave. B factors (Å ²)	
• Protein	20.92
• Sulfate	52.93
• Cl	46.82
• Water	32.23
Ramachandran plot	
• Favored region	98.57
• Allowed regions	1.17
• Outlier regions	0.27

Figure Legends

Figure 1. Characterization of *P. aeruginosa* GlnRS. (A) *P. aeruginosa* GlnRS was titrated into the aminoacylation assay as described in “Methods and Materials” at concentrations between 0.005 and 0.5 μM . Background activity was minimal and was subtracted from values at all concentrations of GlnRS. (B) ATP:PP_i exchange reaction to determine the requirement for the cognate tRNA in the formation of an aminoacyl adenylate by *P. aeruginosa* GlnRS. The reactions contained 0, 0.3, 0.6, 1.2 μM tRNA^{Gln} in lanes 1, 2, 3, and 4, respectively. (C) Determination of the kinetic parameters with respect to tRNA^{Gln} for *P. aeruginosa* GlnRS in the aminoacylation reaction. Initial velocities were determined and the data were fit to a Michaelis-Menten steady-state model using XLfit (IDBS) to determine K_m and V_{max} .

Figure 2. The crystal structure of *P. aeruginosa* GlnRS. (A) The 3-dimensional structure of *P. aeruginosa* GlnRS was solved to 1.9 Å resolution (PDB ID: 5BNZ) as a single α_2 homodimer in the asymmetric unit. (B) Each monomer contained five distinct domains: dinucleotide fold domain (DNF) (blue), acceptor stem binding domain (ABD) (green), helical sub-domain (magenta), proximal beta-barrel (salmon), and distal beta-barrel (yellow).

Figure 3. Amino acid sequence alignment of *P. aeruginosa* and *E. coli* GlnRS. The protein sequences were downloaded from the National Center for Biotechnology Information (NCBI). Accession numbers for GlnRS protein sequences of *E. coli* and *P. aeruginosa* are P00962 and

Q9I2U8, respectively. Sequence alignments were performed using Vector NTI Advance (TM) 11.5.3 (Invitrogen). Identical amino acid residues are white letters on black background and similar residues are black letters on grey background. The positions of the HIGH and KMSKS motifs are boxed. Amino acid residues that interact with Gln (◆), ATP (●) and tRNA (■/□, acceptor stem/anticodon) are indicated.

Figure 4. Comparison of the active site structures of *P. aeruginosa* and *E. coli* GlnRS. In the overlay, *P. aeruginosa* GlnRS is shown in blue and *E. coli* GlnRS is shown in magenta. The aminoacyl adenylate mimic (Gln-AMS) backbone is shown in green and the acceptor stem of tRNA^{Gln} is shown in gold. Amino acid residues interacting with the two substrates are labeled (*P. aeruginosa*/*E. coli* numbering).

Figure 5. Comparison of the anticodon binding regions of GlnRS from *P. aeruginosa* and *E. coli*. In the overlay, *P. aeruginosa* GlnRS is shown in blue and *E. coli* GlnRS is shown in magenta. The three nucleotides forming the anticodon of the tRNA are labeled (C34, U35, and G36). The anticodon of tRNA^{Gln} is shown in gold. Amino acid residues interacting with the nucleotides forming the anticodon are labeled (*P. aeruginosa*/*E. coli* numbering).

Figure 6. Screening assay development. (A) Effect of DMSO in the *P. aeruginosa* GlnRS aminoacylation assay. DMSO (0-10%) was added into the aminoacylation assay described in the

“Chemical Compound Screening” section of “Methods and Materials”. **(B)** To determine the tRNA concentration to be used in screening assays and to determine that the amount of tRNA^{Gln} used would be within the linear region of the reaction-detection time, tRNA was added into the aminoacylation assay described in the “Chemical Compound Screening” section of “Methods and Materials”. The activity was monitored using SPA technology.

Figure 7. The chemical structure of the hit compounds. The structure of **(A)** BM02E04, **(B)** BM04H03, and **(C)** BM04B05.

Figure 8. Determination of the IC₅₀ values of the hit compounds. IC₅₀ values for the inhibitory potency of **(A)** BM02E04, **(B)** BM04B05, and **(C)** BM04H03 against the aminoacylation activity of *P. aeruginosa* GlnRS were 1.9 μM, 2.5 μM, and 40 μM, respectively. The compounds were serially diluted from 200 μM to 0.4 μM into aminoacylation assays containing *P. aeruginosa* GlnRS at 0.12 μM. The “% Positive” indicates the percent of activity observed relative to activity in assays where only DMSO was added to the assay in the absence of compound. The curve fits and IC₅₀ values were determined using the Sigmoidal Dose-Response Model in *XLfit* 5.3 (IDBS).

Figure 9. Activity of BM02E04 and BM04H03 in microbiological assays. The activity of the hit compounds against the growth of cultures containing **(A)** *S. aureus*, and **(B)** *M. catarrhalis*

bacteria were determined using broth microdilution susceptibility testing. Compounds were added to bacterial cultures at 4×MIC. Samples were analyzed by plating and determination of colony forming units (CFU) at 0, 2, 4, 6 and 24 h. Diamonds (◆) represent cultures containing BM04H03 and squares (■) represent cultures containing BM02E04. Circles (●) represent growth of control cultures containing only DMSO in the absence of compound. Toxicity of (C) BM02E04 and (D) BM04H03 were measured using human embryonic kidney 293 (HEK-293) cell cultures. The compound concentrations ranged from 25 to 400 µg/ml. The data points represents an average value for assays carried out in triplicate. The “% Positive” indicates the percent of cell growth observed relative to growth in assays where only DMSO was added to the cells in the absence of compound.

Figure 1

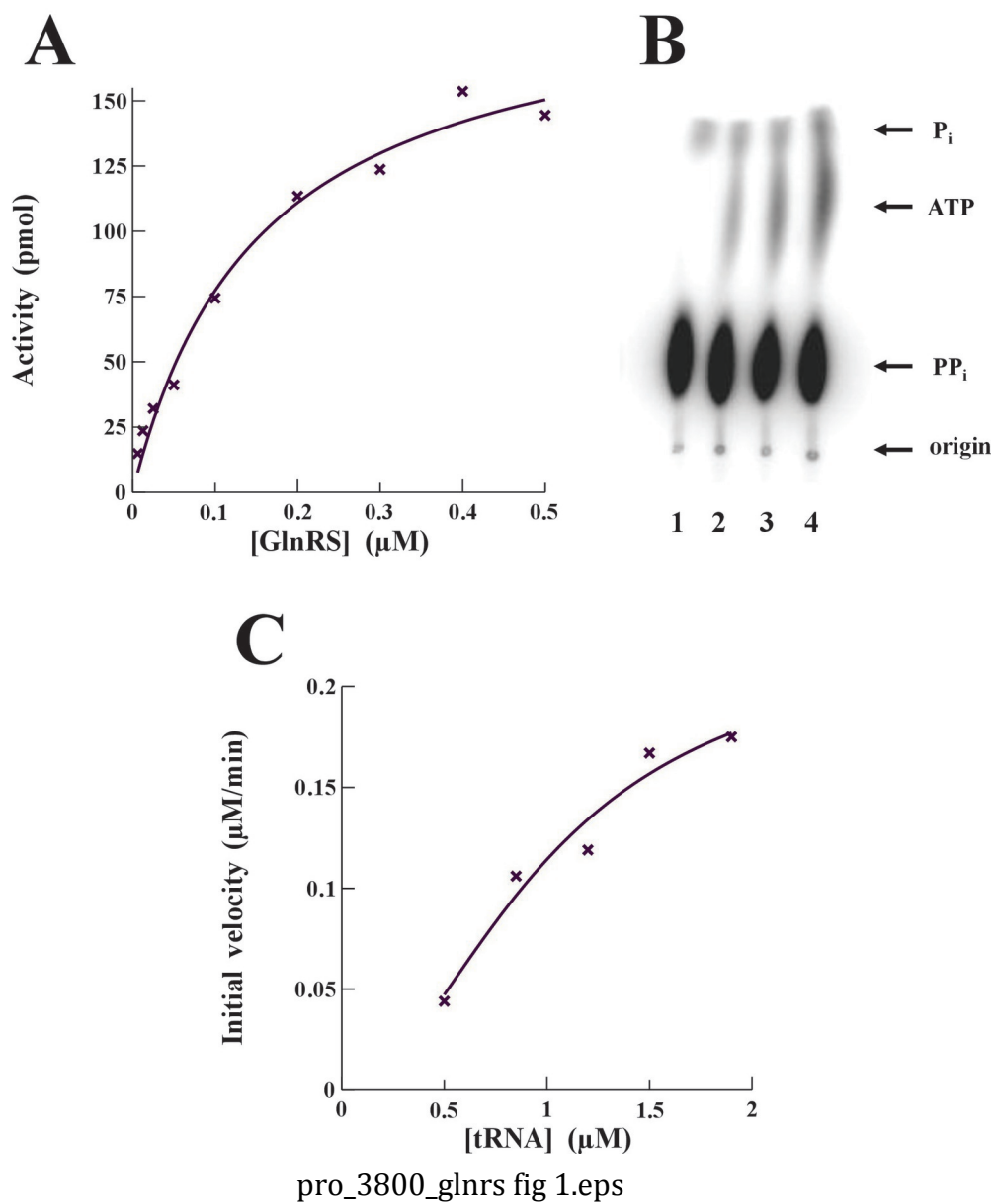
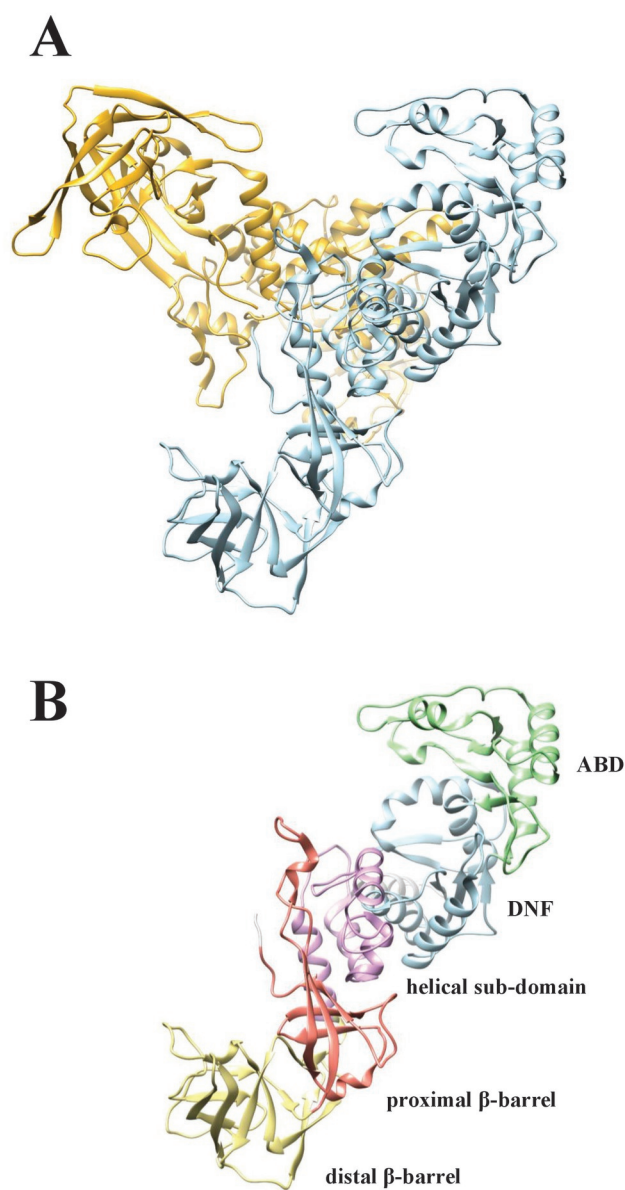
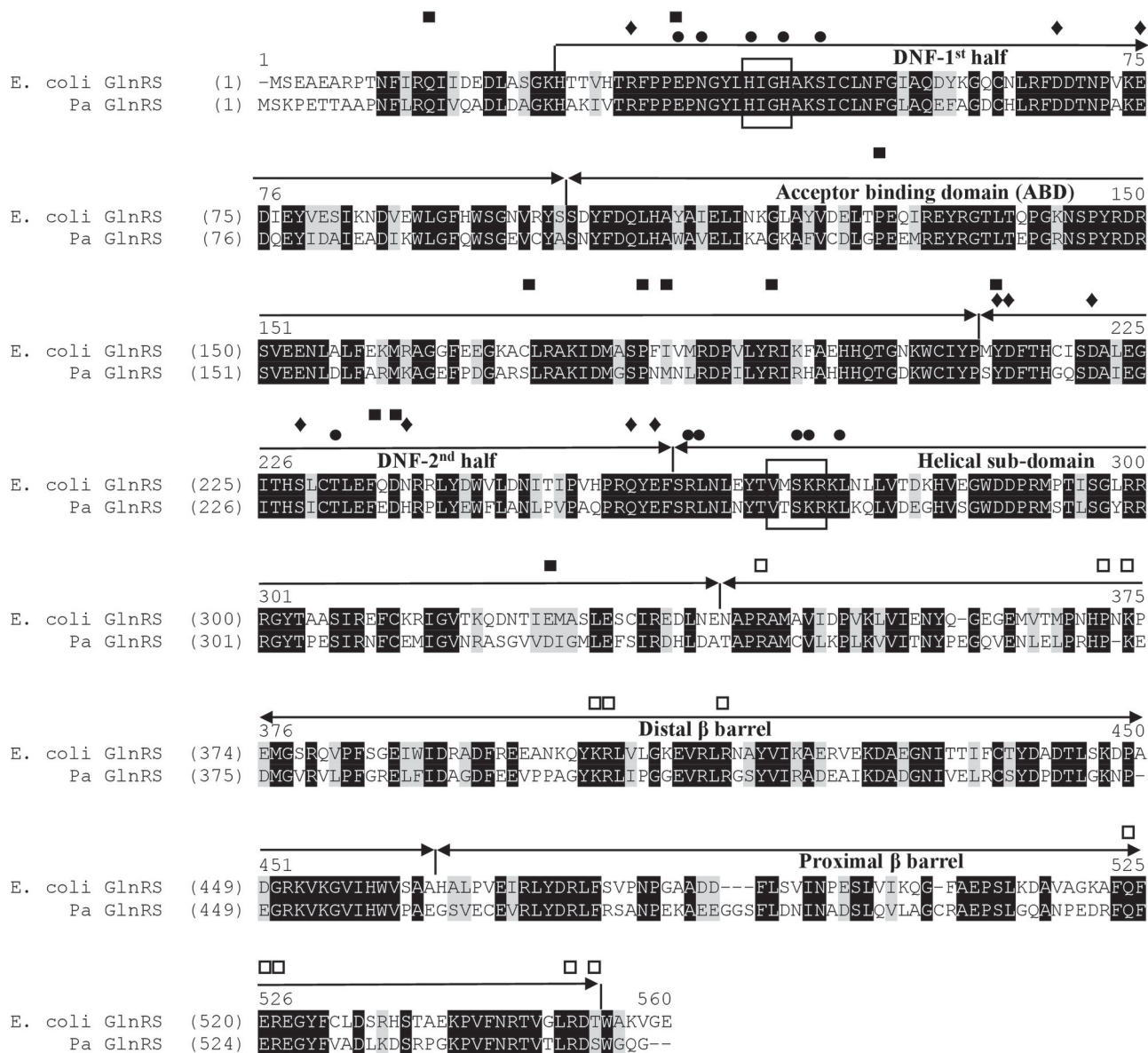


Figure 2



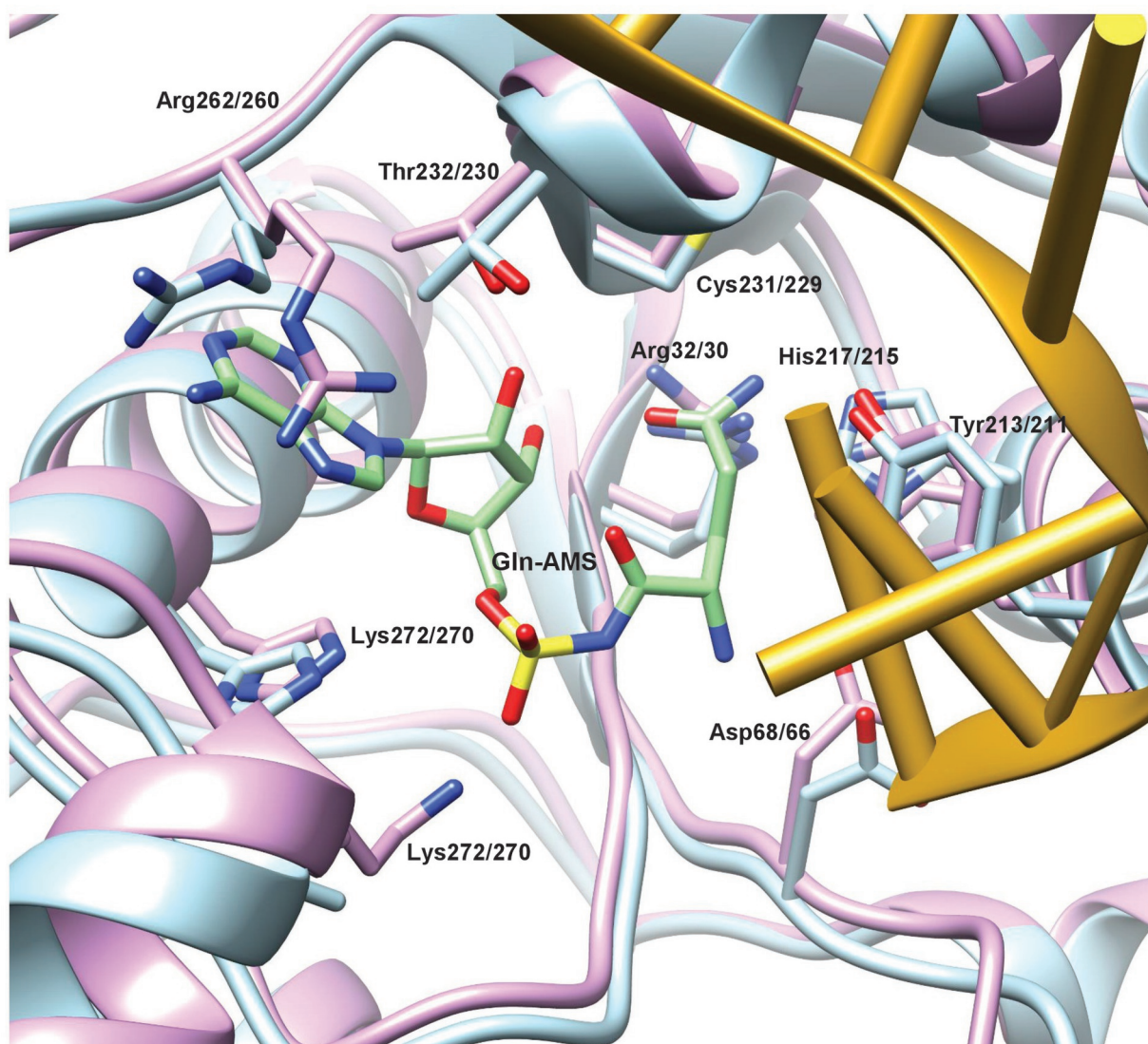
pro_3800_glnrs fig 2.eps

Figure 3



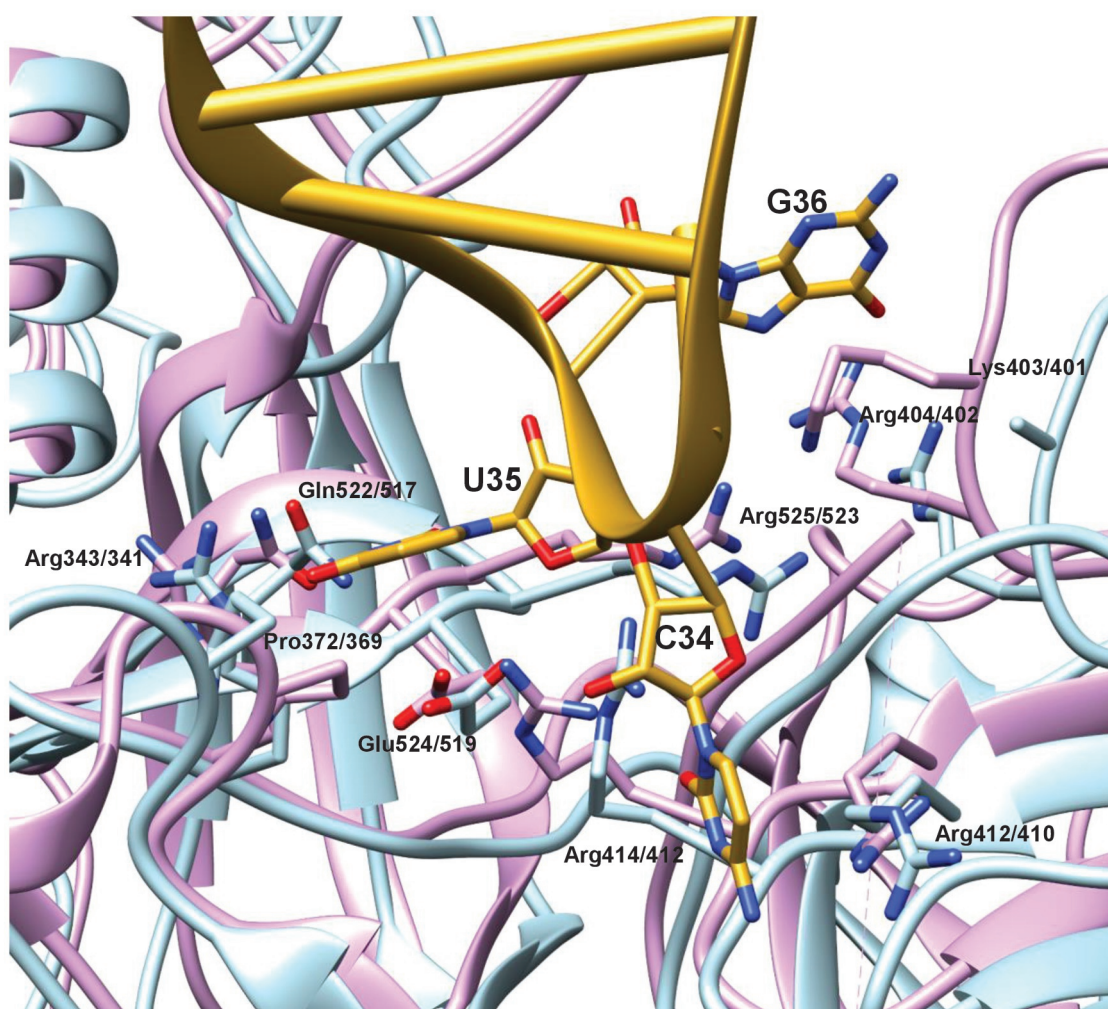
pro_3800_glnrs fig 3.eps

Figure 4



pro_3800_glnrs fig 4.eps

Figure 5



pro_3800_glnrs fig 5.eps

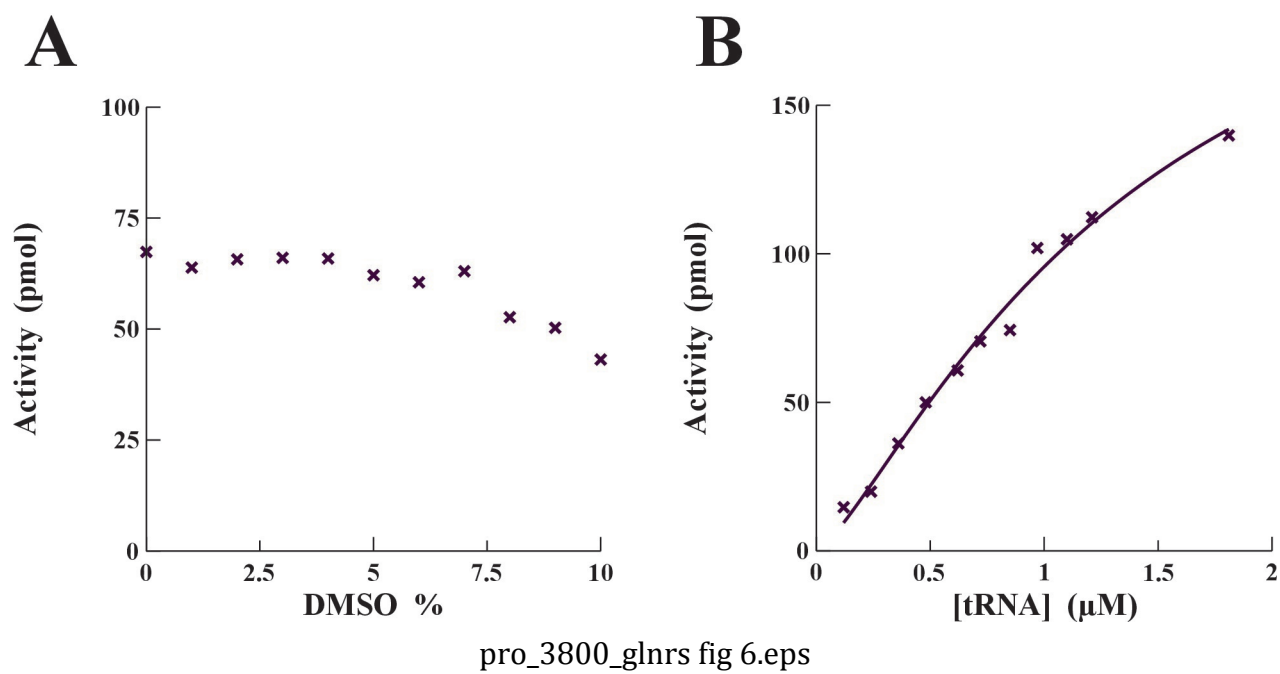
Figure 6

Figure 7

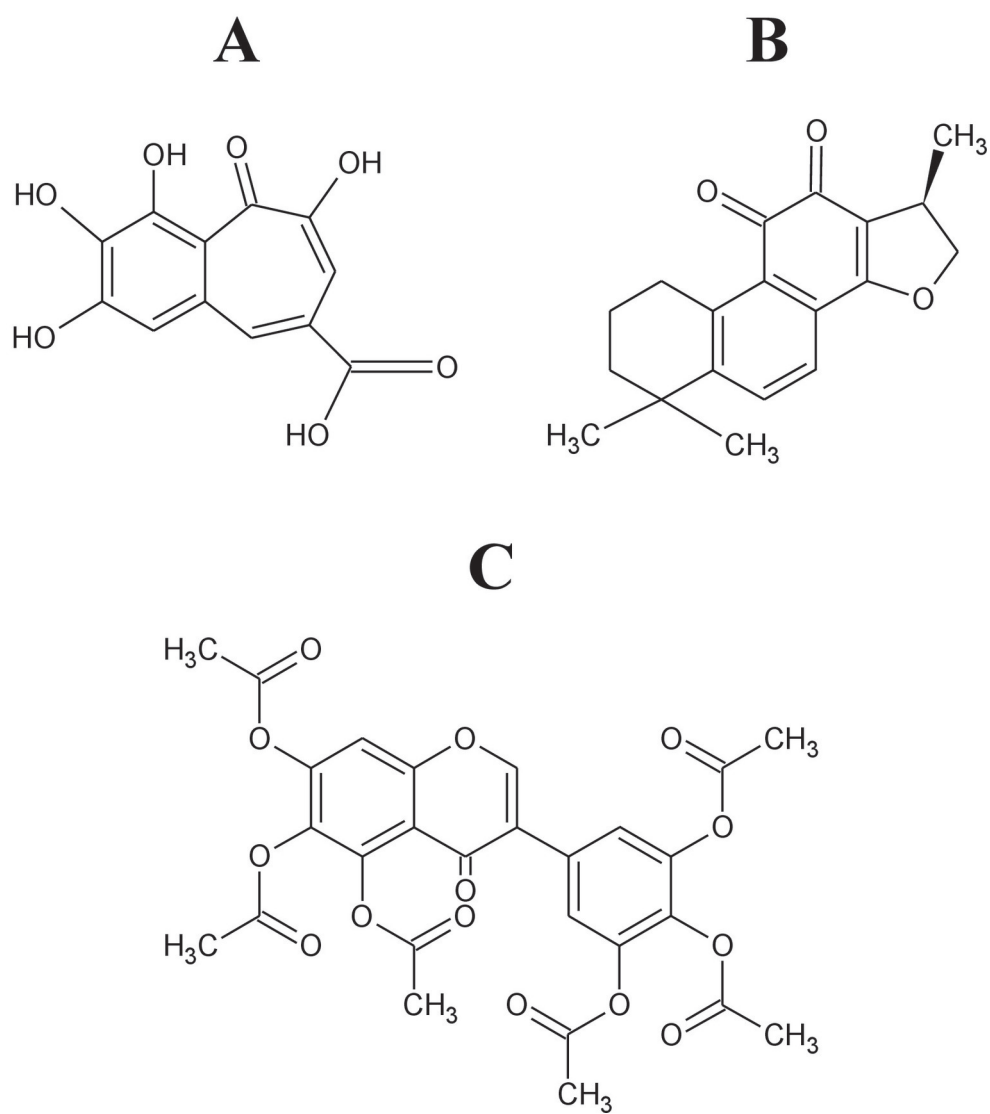
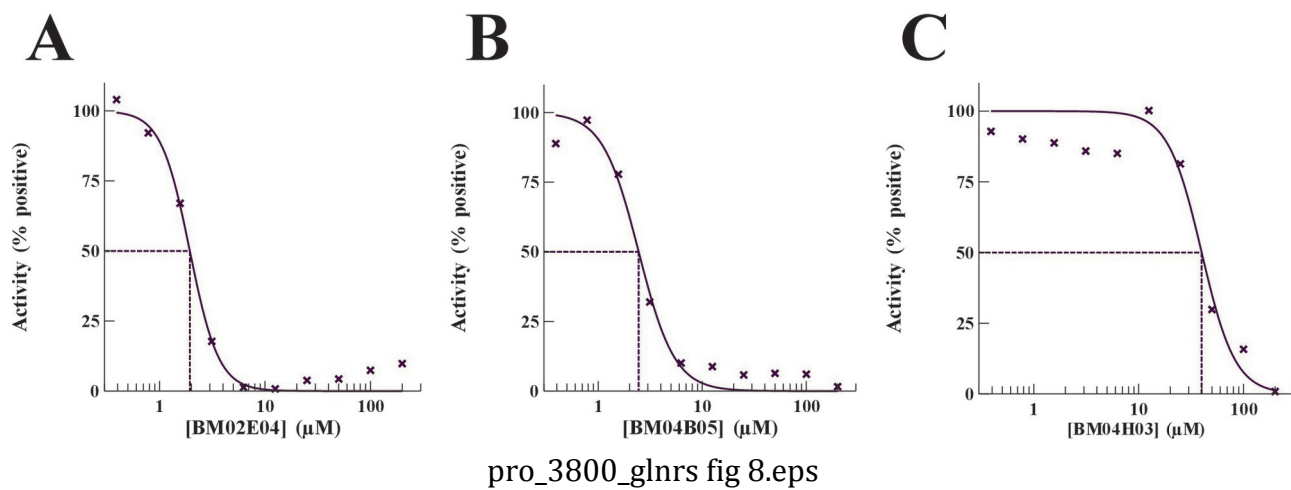
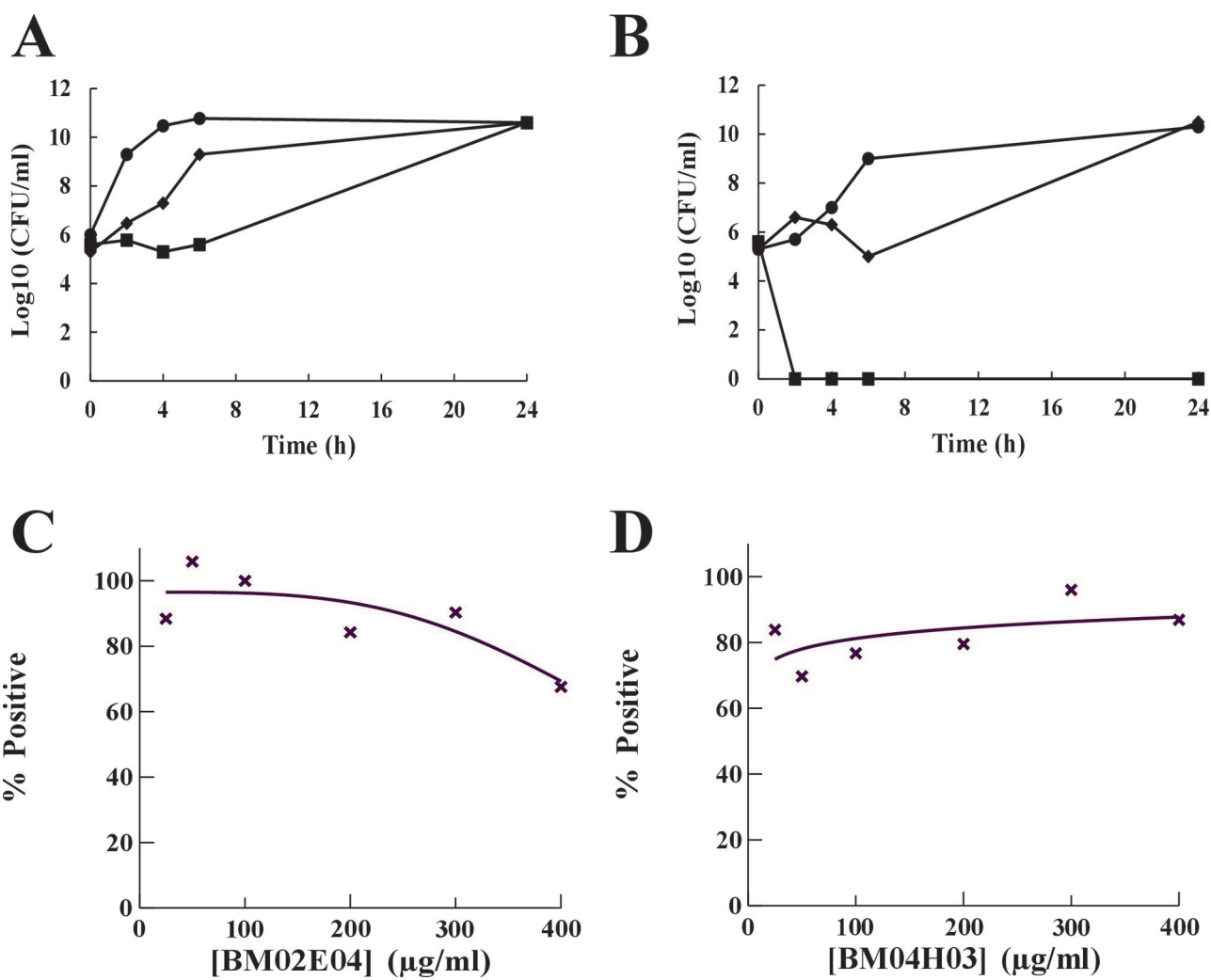


Figure 8



pro_3800_glnrs fig 8.eps

Figure 9



pro_3800_glnrs fig 9.eps